Monthly Notices
of the
ROYAL ASTRONOMICAL SOCIETY

MNRAS **489,** 3643–3647 (2019) doi:10.1093/mnras/stz2386
Advance Access publication 2019 August 29

Non-detection of fast radio bursts from six gamma-ray burst remnants with possible magnetar engines

Yunpeng Men [1,2,3] Kshitij Aggarwal,[4,5] Ye Li,[1] Divya Palaniswamy,[3] Sarah Burke-Spolaor,[4,5⋆] K. J. Lee,[1⋆] Rui Luo [1,2,6] Paul Demorest,[7] Shriharsh Tendulkar,[8] Devansh Agarwal,[4,5] Olivia Young[4,5] and Bing Zhang[3⋆]

[1]Kavli Institute for Astronomy and Astrophysics, Peking University, Beijing 100871, China
[2]Department of Astronomy, School of Physics, Peking University, Beijing 100871, China
[3]Department of Physics and Astronomy, University of Nevada Las Vegas, NV 89154, USA
[4]Department of Physics and Astronomy, West Virginia University, Morgantown, WV 26505, USA
[5]Center for Gravitational Waves and Cosmology, West Virginia University, Chestnut Ridge Research Building, Morgantown, WV 26505, USA
[6]CSIRO Astronomy and Space Science, Australia Telescope National Facility, Box 76, Epping, NSW 1710, Australia
[7]National Radio Astronomy Observatory, Socorro, NM 87801, USA
[8]Department of Physics and McGill Space Institute, McGill University, 3600 University Street, Montreal, QC H3A 2T8, Canada

Accepted 2019 August 27. Received 2019 August 27; in original form 2019 August 7

ABSTRACT

The analogy of the host galaxy of the repeating fast radio burst (FRB) source FRB 121102 and those of long gamma-ray bursts (GRBs) and superluminous supernovae (SLSNe) has led to the suggestion that young magnetars born in GRBs and SLSNe could be the central engine of repeating FRBs. We test such a hypothesis by performing dedicated observations of the remnants of six GRBs with evidence of having a magnetar central engine using the Arecibo telescope and the Robert C. Byrd Green Bank Telescope (GBT). A total of ∼20 h of observations of these sources did not detect any FRB from these remnants. Under the assumptions that all these GRBs left behind a long-lived magnetar and that the bursting rate of FRB 121102 is typical for a magnetar FRB engine, we estimate a non-detection probability of 8.9×10^{-6}. Even though these non-detections cannot exclude the young magnetar model of FRBs, we place constraints on the burst rate and luminosity function of FRBs from these GRB targets.

Key words: telescopes – gamma-ray burst: general.

1 INTRODUCTION

Fast radio bursts (FRBs) are bright millisecond radio pulses with dispersion measure (DM) in excess of the Galactic contribution along the line of sight (Lorimer et al. 2007; Petroff et al. 2016). At least two FRB sources (FRB 121102 and FRB 180814) are found to repeat (Spitler et al. 2014; Scholz et al. 2016; Amiri et al. 2019), suggesting a non-catastrophic progenitor system at least for some FRBs. FRB 121102 was localized in a host galaxy with a redshift $z = 0.19273(8)$ (Tendulkar et al. 2017), confirming the cosmological origin of FRBs. Whether or not all FRBs are repeating sources is subject to debate (Palaniswamy, Li & Zhang 2018; Caleb et al. 2019; Katz 2019). In the literature, the FRB progenitor models can be grouped into two categories: the non-catastrophic models (related to repeating FRBs) such as giant magnetar flares (e.g. Kulkarni et al. 2014; Katz 2016), giant pulses from young pulsars or magnetars (e.g. Popov & Postnov 2010; Connor, Sievers & Pen 2016; Cordes & Wasserman 2016; Murase, Kashiyama & Mészáros 2016; Kashiyama & Murase 2017; Metzger, Berger & Margalit 2017; Margalit & Metzger 2018), and interacting models (e.g. Zhang 2017) among others; and the catastrophic models (related to non-repeating FRBs) such as collapse of supramassive neutron stars (Falcke & Rezzolla 2014; Zhang 2014) and mergers of compact stars (e.g. Totani 2013; Wang et al. 2016; Zhang 2016; Liu et al. 2016). See Platts et al. (2018) for a complete list of FRB progenitor models.

Gamma-ray bursts (GRBs) are most luminous explosions in the Universe, signalling core collapse of massive stars or mergers of compact objects (Mészáros 2006; Zhang 2018). They are much rarer than FRBs. However, the following theoretical arguments have been made to suggest that a small fraction of FRBs could be associated with GRBs for different reasons: (1) A good fraction of both long and short GRBs have an X-ray plateau followed by a rapid decay, which are best interpreted as a supramassive neutron star collapsing to a BH at $\sim(10^2 - 10^4)$ s after the GRB triggers (Troja et al. 2007; Rowlinson et al. 2010, 2013; Lü & Zhang 2014; Lü et al. 2015). If FRBs are produced from the so-called 'blitzar' scenario (Falcke & Rezzolla 2014), an FRB would be produced with such a delay

⋆ E-mail: sarah.spolaor@mail.wvu.edu (SB-S); kjlee@pku.edu.cn (KJL); zhang@physics.unlv.edu (BZ)

Table 1. The parameters of the observed target GRBs and observations.

GRB name[a] (yymmdd)	Redshift	RA (h : m : s)	Dec. (° : ′ : ″)	DM_{IGM} (cm^{-3} pc)	DM_{MW}[b] (cm^{-3} pc)	Obs. telescope	Obs. time (min)	Comments
030329	0.168	10:44:50.00	+ 21:31:17.8	147	17	Arecibo	340.7	LGRB + SN2003dh
130603B	0.3564	11:28:48.16	+ 17:04:18.0	311	29	Arecibo	448.8	short GRB
111225A	0.297	00:52:37.21	+ 51:34:19.5	259.875	118.09	GBT	76.5	LGRB
051109B	0.08	23:01:50.30	+ 38:40:46.7	70.0	71.17	GBT	131.3	LGRB
111005A	0.013	14:53:07.74	−19:44:08.9	11.375	51.12	GBT	82.5	LGRB
980425	0.0085	13:25:41.93	−26:46:55.7	7.43	53.59	GBT	70.6	LGRB + SN1998bw

[a]GRB targets with data damaged are not listed.
[b]DM_{MW} is Galactic contribution to the overall DM, which is estimated by integrating the NE2001 model (Cordes & Lazio 2002) to the edge of the Galaxy.

time after these GRBs (Zhang 2014); (2) If a small fraction of non-repeating FRBs are related to mergers of binary neutron stars (Totani 2013), it is possible that an FRB may be associated with a short GRB (e.g. Wang et al. 2016; Zhang 2016); (3) If FRBs are produced when the magnetosphere of a neutron star is reconfigured by an external astrophysical stream, a GRB could be the source of the astrophysical stream to trigger FRBs (Zhang 2017); (4) Within the young magnetar model for repeating FRBs (e.g. Metzger et al. 2017; Margalit & Metzger 2018), a GRB could be the progenitor of the young magnetar that later produce FRBs. Such a connection is promising in view of the similarity of the host galaxy of FRB 121102 (a dwarf star-forming galaxy at redshift $z = 0.19273(8)$, Chatterjee et al. 2017; Marcote et al. 2017; Tendulkar et al. 2017), to those of long GRBs and superluminous supernovae (SLSNe) (Metzger et al. 2017; Nicholl et al. 2017; Tendulkar et al. 2017). Moreover, Eftekhari et al. (2019) showed tentative evidence for a radio source coincident with the SLSNe PTF10hgi, similar to that of FRB 121102 (Chatterjee et al. 2017; Marcote et al. 2017; Tendulkar et al. 2017), which could be produced by a magnetar central engine. Within such a picture, a GRB should proceed the repeating FRBs by months to decades.

Searching for GRB–FRB associations have been carried out in the past to test the first three hypothesis so far with null results (Bannister et al. 2012; Palaniswamy et al. 2014; DeLaunay et al. 2016; Cunningham et al. 2019; Guidorzi et al. 2019). More dedicated searches for GRBs around the time of FRBs, and for FRBs following GRBs (especially short GRBs) within <100 s of the burst triggers are encouraged in order to rule out these possibilities.

In this work, we test the fourth hypothesis of GRB/FRB associations, which is related to repeating FRBs. So far, only two repeating FRBs have been reported in the literature, FRB 121102 (Scholz et al. 2016; Spitler et al. 2016) and FRB 180814 (Amiri et al. 2019). Searching for GRBs from archival Fermi data have been carried out for these two sources with null results (Yamasaki, Totani & Kawanaka 2016; Zhang & Zhang 2017; Xi et al. 2017; Yang, Zhang & Zhang 2019). We adopt an opposite approach. We first identify several historical GRBs likely having a magnetar central engine based on their light curves. We then perform dedicated searches for FRBs from these GRB remnants using the Arecibo telescope and the Robert C. Byrd Green Bank Telescope (GBT). The total search time is about 20 h. No FRBs have been detected. We present the details of our observations and data analysis results in Sections 2 and 3, respectively. The implications of our results on FRB progenitor systems are presented in Section 4, and the conclusions are summarized in Section 5.

2 OBSERVATIONS

The observations were performed with the Arecibo and GBT. Each telescope was pointed at different GRB remnants multiple times. The parameters of target GRBs are listed in Table 1. These target GRBs were selected based on three criteria: (1) They are nearby GRBs with $z < 0.4$; (2) They fall into the declination ranges of the telescopes; (3) Four of them show an X-ray light-curve plateau signature consistent with the magnetar central engine criteria as defined in Lü & Zhang (2014). Two famous pre-*Swift* nearby long GRBs, GRB 980425 (Galama et al. 1998) and GRB 030329 (Hjorth et al. 2003), are also selected. These two GRBs have Type Ic SN associations and have been suggested to be powered by magnetars (Mazzali et al. 2014). Among the six sources, one source, GRB 130603B, is a short GRB, whose X-ray light curve and the kilonova signature can be self-consistently interpreted as being powered by a magnetar central engine (Fan et al. 2013). The newly localized FRB 180924 (Bannister et al. 2019) has an environment consistent with that of a short GRB, justifying search for FRBs from short GRBs like GRB 130603B. The other five GRBs are all long GRBs. The ages of these GRBs range from 20 (GRB 980425) to 5 yr (GRB 111225A), which fall into the suggested magnetar age range that is favourable for FRB production and detection (Metzger et al. 2017).

2.1 Arecibo

Four GRB sources were observed for 25 one-hour durations at Arecibo, but unfortunately, most of the data were damaged in the Hurricane Maria and only about 10 h of data from two GRB targets (long GRB 030329 and short GRB 130603B) are available, as shown in Table 1.

The observations were conducted with the single-pixel L-wide receiver. The central frequency of the observations is 1440 MHz and the bandwidth is 580 MHz. The system temperature T_{sys} is 30 K and the gain G is 10.5 K Jy^{-1}. The minimum detectable flux is

$$S_{min} = \beta \frac{\gamma \, T_{sys}}{G \sqrt{BW \, \tau \, N_p}}, \quad (1)$$

where γ is the threshold of signal-to-noise ratio (S/N), $\beta \simeq 1$ is the digitization factor, BW is the bandwidth, N_p is the number of polarizations, and τ is the pulse width. By choosing 3 ms as the reference width of a possible FRB, the flux thresholds for S/N > 7 is 10.7 mJy. The data were recorded with the PUPPI backend in incoherent search mode with a 800 MHz total bandwidth, 2048 frequency channels, 256 µs time resolution, and the summed polarization.

2.2 Green Bank Telescope

Four long GRB sources (GRBs 980425, 052209B, 111005, and 111225) were observed at GBT, as listed in Table 1. The observational times of the target GRBs are listed in Table 1.

The observations were performed with the 820 MHz and 2 GHz receivers. The system temperature is T_{sys} of 25 K and the gain is

2 K Jy^{-1}, which yields the minimum detectable flux of 38.3 mJy according to equation (1). We recorded the observation data with the GUPPI backend in the search mode, in which nominal 800 MHz bands are sampled with 256 µs time resolution and 2048 spectral channels. The data are polarization summed.

3 DATA REDUCTION AND RESULTS

The observation data are processed with the pipeline 'Burst Emission Automatic Roger' (BEAR) which is used to search for dispersed burst signals (Men et al. 2019). The raw data are first normalized with zero mean and unit variance in each frequency channel. We perform the radio frequency interference (RFI) mitigation using the *zero-DM matched filter*, which estimates the waveform of the zero DM signal and subtracts only the corresponding contribution from each frequency channel (Men et al. 2019). The data are then dedispersed with trial DMs ranging from 0 to 1000 cm^{-3} pc with a DM step 0.1 cm^{-3} pc. The maximum DM searched is roughly twice as high as the estimated IGM and Milky Way contributions to DM listed in Table 1. The DM step gives a smearing compared to the time resolution. We then search for burst signals in the dedispersed time series using the *matched filter* that convolves the dedispersed time series with a series of boxcar matched filters with a geometric series of width covering 0.256–20 ms. The burst candidates with S/N > 7 are saved, while the duplicated candidates are removed using the candidate clustering algorithm (for a general discussion, see Men et al. 2019).

Before reducing the data from the GRB remnants, we test the search pipeline with the test observation data of PSR B1133+16 at Arecibo. All the single pulses of PSR B1133 + 16 can be detected with BEAR. After the burst signal search in the data, about 23 000 and 900 candidates were reported by BEAR in the Arecibo and GBT data, respectively. We scan all the candidates with eyes and they are all recognized as RFI signals. As a result, we have no positive detection of celestial bursts in the data.

The data were also processed using Graphics Processing Unit (GPU) accelerated transient detection pipeline HEIMDALL[1] (Barsdell et al. 2012). The parameters used in the search were: S/N > 6, 20 ≤ DM ≤ 10 000 pc cm^{-3}, and width ≤32 ms. This resulted in 27 779 candidates which were then classified using model a of the deep learning based classifier FETCH[2] (Agarwal et al. 2019) to identify FRBs from RFI. It identified 305 candidates as potential FRBs, which were then visually inspected and found to be RFI.

4 TESTING THE YOUNG MAGNETAR MODEL FOR FRBS

4.1 Non-detection probability

The non-detection of FRBs from these GRB remnants can be used to test the young magnetar – FRB association hypothesis.

We can estimate the non-detection probability from our observations based on three assumptions: (1) FRB 121102 burst rate is typical for repeating FRB sources that host a young magnetar; (2) The distribution of the number of bursts n in a given duration T is Poissonian, i.e.

$$P(n|T,\eta) = \frac{(\eta T)^n \, e^{\eta T}}{\Gamma(n+1)}\,, \quad (2)$$

[1] https://sourceforge.net/projects/heimdall-astro/
[2] https://github.com/devanshkv/fetch

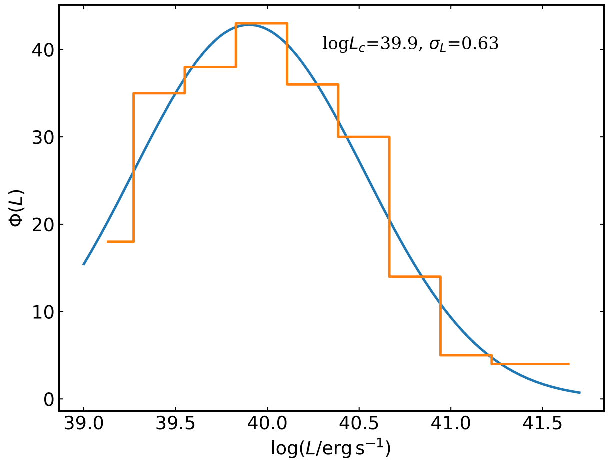

Figure 1. The luminosity distribution of the bursts of FRB 121102 reported currently. The luminosity are derived using equation (5) with $z = 0.19273$. We choose a characteristic bandwidth of 200 MHz (Gourdji et al. 2019). The best fitting using equation (3) gives $\log L_c = 39.9$ and $\sigma_L = 0.63$.

where η is the intrinsic burst rate; (3) the luminosity function of the bursts $\Phi(L)$ for an FRB source is Gaussian logarithm, i.e.

$$\Phi(L|L_c,\sigma_L) = \frac{1}{\sqrt{2\pi}\sigma_L\, L} e^{-\frac{1}{2}\left[\log\left(\frac{L}{L_c}\right)/\sigma_L\right]^2}\,, \quad (3)$$

where L_c is the peak luminosity and σ_L is the standard deviation of $\log L$. This last assumption is based on the luminosity distribution statistics of 227 bursts detected from FRB 121102 (Spitler et al. 2014, 2016; Scholz et al. 2016, 2017; Hardy et al. 2017; Law et al. 2017; MAGIC Collaboration 2018; Michilli et al. 2018; Spitler et al. 2018; Zhang et al. 2018; Gourdji et al. 2019; Hessels et al. 2019), as shown in Fig. 1.

With the above assumptions, the non-detection probability of FRBs from these targets can be written as

$$P_{\rm non}(\eta, L_c, \sigma_L) = 1 - P(n>0|T,\eta)\int_{L_{\rm min}}^{\infty}\Phi(L|L_c,\sigma_L)\mathrm{d}L\,, \quad (4)$$

with

$$L_{\rm min} = 4\pi\, r_{\rm L}^2(z)\, {\rm BW}\, S_{\rm min}\,. \quad (5)$$

The luminosity distance $r_L(z)$ at the redshift z is defined as

$$r_{\rm L}(z) = \frac{c(1+z)}{H_0}\int_0^z \frac{1}{E(z)}\mathrm{d}z\,, \quad (6)$$

where the Hubble constant $H_0 = 67.8$ km s^{-1} Mpc^{-1} (Planck Collaboration VI 2018), and c is the light speed. $E(z)$ is the logarithmic time derivative of the cosmic scale factor, which is defined as

$$E(z) = \sqrt{\Omega_{\rm m}(1+z)^3 + \Omega_\Lambda}\,, \quad (7)$$

where the total matter density $\Omega_m = 0.308$ and the dark energy density $\Omega_\Lambda = 0.692$ have been adopted (Planck Collaboration VI 2018).

We conservatively determine the parameters of FRB 121102 using the data in Li et al. (2019b), who summarized the burst data of FRB 121102 and exhibited the statistical properties of the bursts. We adopt the observed burst rate $\eta = 3\,h^{-1}$ as the intrinsic rate. The two luminosity function parameters $L_c = 10^{39.9}$ erg s^{-1} and $\sigma_L = 0.63$ are estimated through the flux density distribution with $z = 0.19273$ for FRB 121102, as shown in Fig. 1. Using equation (4), the non-detection probability can be determined for each GRB target

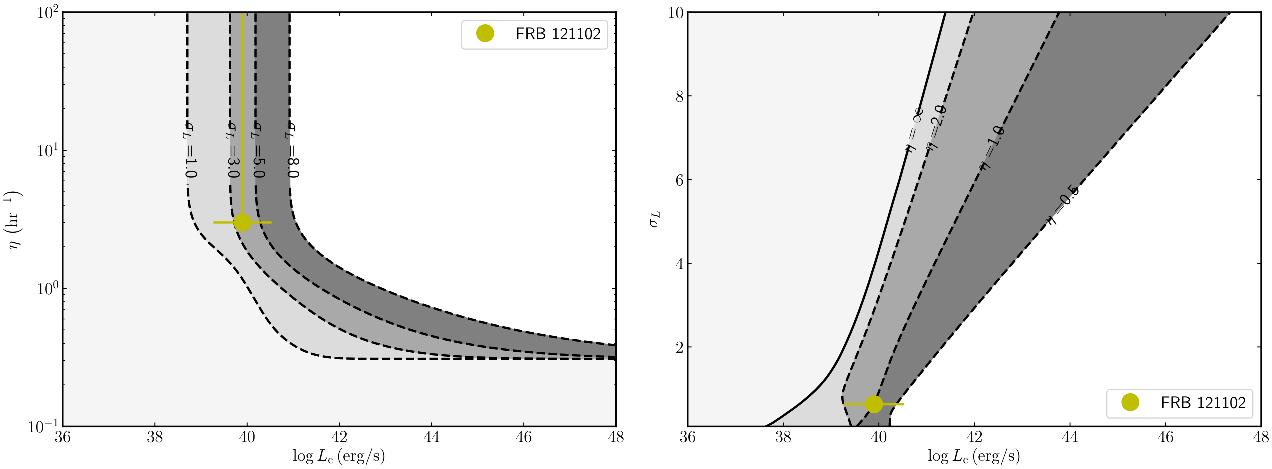

Figure 2. Constraints on the intrinsic burst rate η, the peak luminosity L_c, and the standard deviation of luminosity function σ_L based on the non-detection results with the total non-detection probability of 0.0027. The brighter region allows the existence of parameters. The FRB 121102 with $\eta = 3\,\mathrm{h}^{-1}$, $L_c = 10^{39.9}$ erg s^{-1}, and $\sigma_L = 0.63$ is plotted in the figures. *Left-hand panel:* The constrain region of η and L_c with $\sigma_L = 1, 3, 5, 8$. *Right-hand panel:* The constrain region of σ_L and L_c with $\eta = 0.5, 1, 2, \infty$.

with the observational time and redshift in Table 1. The total non-detection probability of all targets is the product of each one, which is 8.9×10^{-6}.

Such a low probability may be regarded as evidence disfavouring the possibility that GRB remnants with a young magnetar engine as the source of repeating FRBs. However, this possibility cannot be ruled out by the data. Possibilities to lower the non-detection probability include: (1) Not all these GRB remnants harbour a magnetar (i.e. the arguments in favour of a magnetar engine are for some reasons unjustified); (2) Maybe some of the young magnetars formed the remnants are supramassive and have collapsed to black holes when our observations started; (3) The supernova ejecta may not yet become transparent to free–free emission at the observing frequency (Margalit et al. 2018 showed that the time-scales for free–free transparency of the ejecta can vary from decades to up to a 100 yr); (4) The synchrotron self-absorption by a flare-powered nebula may dominate the radiative processes; (5) FRB 121102 bursts are sporadic, and there are quiescent period (e.g. Price et al. 2018); (6) FRB 121102 source is abnormally active compared with most young magnetars, as have been also suggested in previous studies (Palaniswamy et al. 2018; Caleb et al. 2019).

4.2 Constraints on the intrinsic burst rate and luminosity function

In the following we assume that the non-detection is caused by the last two reasons discussed above and constrain the intrinsic FRB burst rate and luminosity function of young magnetars. By doing so, we have assumed that all these GRB remnants harbour young magnetars and they are still alive at the time of our observations. We have also made the assumptions (2) and (3) made in Section 4.1.

Using equation (4), the constraints on the intrinsic burst rate and luminosity function can be inferred by choosing the non-detection probability of 0.0027, which equals to 3σ significance. Here we give the $\eta - L_c$ curve with $\sigma_L = 1, 3, 5, 8$, and $\sigma_L - L_c$ curve with $\eta = 0.5, 1, 2, \infty$. The results are shown in Fig. 2, in which the allowed regions are to the left of the contours. We also place FRB 121102 with $\eta = 3\,\mathrm{h}^{-1}$, $L_c = 10^{39.9}$ erg s^{-1}, and $\sigma_L = 0.63$ in the plot. More extensive searches of FRBs from similar targets in the future can tighten these constraints further.

5 CONCLUSIONS AND DISCUSSION

We have performed dedicated searches of FRBs from six nearby historical GRB sources (five long and one short) which are consistent with having a millisecond magnetar central engine. The motivation is to test the hypothesis that these young magnetars born from GRB remnants can be the sources of repeating FRBs, as suggested by the similarity between the host galaxy of FRB 121102 and those of long GRBs (Metzger et al. 2017; Nicholl et al. 2017; Tendulkar et al. 2017). Our 20 h observations with Arecibo and GBT did not detect any FRB from these sources.

Under the assumptions that these sources indeed harbour magnetars similar to the putative magnetar that is powering FRB 121102, that the burst rate is Poissonian, and that the luminosity function is Gaussian logarithmic, we conservatively estimated the non-detection probability of FRB 121102-like bursts to be 8.9×10^{-6}. This result challenges the young magnetar scenario to power FRBs, even though the scenario cannot be ruled out. Assuming that the young magnetars still exist in these remnants and that they indeed produce FRBs without free–free absorption or synchrotron self-absorption, we place the constraints on the burst rate and luminosity function based on the non-detection observations.

Recent localizations of FRB 180924 (Bannister et al. 2019) and FRB 190523 (Ravi et al. 2019) suggest that the host galaxy of FRB 121102 is not the norm of FRB hosts. A survey of possible host galaxies of nearby (excess DM < 100) FRBs also suggests that the FRB 121102 host is abnormal (Li et al. 2019a). All these suggest that LGRBs and SLSNe are likely not the dominant channel to produce FRB sources, which is consistent with the finding of our paper.

ACKNOWLEDGEMENTS

YPM, KJL, and RL were supported by NSFC U15311243, National Basic Research Program of China, 973 Program, 2015CB857101 and XDB23010200. SB-S and KA acknowledge support from NSF grant AAG-1714897. DA acknowledges support from the NSF awards OIA-1458952 and PHY-1430284. We are grateful to L.J. Zhao and D.Y. Chen for helpful discussion.

REFERENCES

Agarwal D., Aggarwal K., Burke-Spolaor S., Lorimer D. R., Garver-Daniels N., 2019, preprint (arXiv:1902.06343)
Amiri M. et al., 2019, Nature, 566, 235
Bannister K. W., Murphy T., Gaensler B. M., Reynolds J. E., 2012, ApJ, 757, 38
Bannister K. W. et al., 2019, Science, 365, 565
Barsdell B. R., Bailes M., Barnes D. G., Fluke C. J., 2012, MNRAS, 422, 379
Caleb M., Stappers B. W., Rajwade K., Flynn C., 2019, MNRAS, 484, 5500
Chatterjee S. et al., 2017, Nature, 541, 58
Connor L., Sievers J., Pen U.-L., 2016, MNRAS, 458, L19
Cordes J. M., Lazio T. J. W., 2002, preprint (astro-ph/0207156)
Cordes J. M., Wasserman I., 2016, MNRAS, 457, 232
Cunningham V. et al., 2019, ApJ, 879, 40
DeLaunay J. J. et al., 2016, ApJ, 832, L1
Eftekhari T. et al., 2019, ApJ, 876, L10
Falcke H., Rezzolla L., 2014, A&A, 562, A137
Fan Y.-Z., Yu Y.-W., Xu D., Jin Z.-P., Wu X.-F., Wei D.-M., Zhang B., 2013, ApJ, 779, L25
Galama T. J. et al., 1998, Nature, 395, 670
Gourdji K., Michilli D., Spitler L. G., Hessels J. W. T., Seymour A., Cordes J. M., Chatterjee S., 2019, ApJ, 877, L19
Guidorzi C. et al., 2019, ApJ, 882, 100
Hardy L. K. et al., 2017, MNRAS, 472, 2800
Hessels J. W. T. et al., 2019, ApJ, 876, L23
Hjorth J. et al., 2003, Nature, 423, 847
Kashiyama K., Murase K., 2017, ApJ, 839, L3
Katz J. I., 2016, ApJ, 826, 226
Katz J. I., 2019, MNRAS, 487, 491
Kulkarni S. R., Ofek E. O., Neill J. D., Zheng Z., Juric M., 2014, ApJ, 797, 70
Law C. J. et al., 2017, ApJ, 850, 76
Li Y., Zhang B., Nagamine K., Shi J., 2019a, preprint (arXiv:1906.08749)
Li B., Li L.-B., Zhang Z.-B., Geng J.-J., Song L.-M., Huang Y.-F., Yang Y.-P., 2019b, preprint (arXiv:1906.08749)
Liu T., et al., 2016, ApJ, 826, 82
Lorimer D. R., Bailes M., McLaughlin M. A., Narkevic D. J., Crawford F., 2007, Science, 318, 777
Lü H.-J., Zhang B., 2014, ApJ, 785, 74
Lü H.-J., Zhang B., Lei W.-H., Li Y., Lasky P. D., 2015, ApJ, 805, 89
MAGIC Collaboration, 2018, MNRAS, 481, 2479
Marcote B. et al., 2017, ApJ, 834, L8
Margalit B., Metzger B. D., 2018, ApJ, 868, L4
Margalit B., Metzger B. D., Berger E., Nicholl M., Eftekhari T., Margutti R., 2018, MNRAS, 481, 2407
Mazzali P. A., McFadyen A. I., Woosley S. E., Pian E., Tanaka M., 2014, MNRAS, 443, 67
Men Y. P. et al., 2019, MNRAS, 488, 3957
Mészáros P., 2006, Rep. Prog. Phys., 69, 2259
Metzger B. D., Berger E., Margalit B., 2017, ApJ, 841, 14
Michilli D. et al., 2018, Nature, 553, 182
Murase K., Kashiyama K., Mészáros P., 2016, MNRAS, 461, 1498
Nicholl M., Williams P. K. G., Berger E., Villar V. A., Alexander K. D., Eftekhari T., Metzger B. D., 2017, ApJ, 843, 84
Palaniswamy D., Wayth R. B., Trott C. M., McCallum J. N., Tingay S. J., Reynolds C., 2014, ApJ, 790, 63
Palaniswamy D., Li Y., Zhang B., 2018, ApJ, 854, L12
Petroff E. et al., 2016, Publ. Astron. Soc. Aust., 33, e045
Planck Collaboration VI, 2018, preprint (arXiv:1807.06209)
Platts E., Weltman A., Walters A., Tendulkar S. P., Gordin J. E. B., Kandhai S., 2019, in Kamionkowski M.P., ed., Physics Reports: A living theory catalogue for fast radio bursts, Elsevier, Netherlands
Popov S. B., Postnov K. A., 2010, in Harutyunian H. A., Mickaelian A. M., Terzian Y., eds, Evolution of Cosmic Objects through their Physical Activity. Gitutyun Publishing House of NAS RA, Yerevan, p. 129
Price D. C. et al., 2018, Res. Notes Am. Astron. Soc., 2, 30
Ravi V. et al., 2019, Nature, 572, 352
Rowlinson A. et al., 2010, MNRAS, 409, 531
Rowlinson A., O'Brien P. T., Metzger B. D., Tanvir N. R., Levan A. J., 2013, MNRAS, 430, 1061
Scholz P. et al., 2016, ApJ, 833, 177
Scholz P. et al., 2017, ApJ, 846, 80
Spitler L. G. et al., 2014, ApJ, 790, 101
Spitler L. G. et al., 2016, Nature, 531, 202
Spitler L. G. et al., 2018, ApJ, 863, 150
Tendulkar S. P. et al., 2017, ApJ, 834, L7
Totani T., 2013, PASJ, 65, L12
Troja E. et al., 2007, ApJ, 665, 599
Wang J.-S., Yang Y.-P., Wu X.-F., Dai Z.-G., Wang F.-Y., 2016, ApJ, 822, L7
Xi S.-Q., Tam P.-H. T., Peng F.-K., Wang X.-Y., 2017, ApJ, 842, L8
Yamasaki S., Totani T., Kawanaka N., 2016, MNRAS, 460, 2875
Yang Y.-H., Zhang B.-B., Zhang B., 2019, ApJ, 875, L19
Zhang B., 2014, ApJ, 780, L21
Zhang B., 2016, ApJ, 827, L31
Zhang B., 2017, ApJ, 836, L32
Zhang B., 2018, The Physics of Gamma-Ray Bursts, Cambridge Univ. Press, Cambridge
Zhang B.-B., Zhang B., 2017, ApJ, 843, L13
Zhang Y. G., Gajjar V., Foster G., Siemion A., Cordes J., Law C., Wang Y., 2018, ApJ, 866, 149

This paper has been typeset from a TEX/LATEX file prepared by the author.